

Stack design and performance of polymer electrolyte membrane fuel cells

Rongzhong Jiang, Deryn Chu^{*}

U.S. Army Research Laboratory, Sensors and Electron Devices Directorate, Adelphi, MD 20783-1197, USA

Received 24 December 1999; accepted 10 June 2000

Abstract

Three types of stack structure designs of polymer electrolyte membrane electrolyte fuel cells (PEMFCs) were reviewed and evaluated under various humidities and temperatures, including bipolar, pseudo bipolar and monopolar (strip) stacks. The bipolar stack design is suitable for delivering moderate to high power, but if a single cell fails it may lead to a loss of power for the whole stack. Water, heat, fuel and air management is required in bipolar plate design. For the pseudo-bipolar cell stack design it is easy to achieve high power by simple addition of more bi-cell units, but each bi-cell has to be filled with fuel and air separately. In the monopolar cell stack design a common gas flow field is shared by a whole strip, when a single cell fails the stack performance will not be affected seriously. Monopolar cell stack design is suitable for applications in low power and high voltage devices because of its high internal resistance. Published by Elsevier Science B.V.

Keywords: Fuel cell; PEMFC; Fuel cell stack; Stack design; Fuel cell structures

1. Introduction

Direct conversion of fuel to electricity has long been a dream since about 160 years ago when the concept of a fuel cell was conceived [1], which employed hydrogen and oxygen to react through an electrolyte solution. Requirements of modern industry, the military and consumers for clean and inexpensive energy sources have created a new opportunity to research and develop fuel cells for transportation, portable computer, cellular phone and information storage. Among many kinds of fuel cells, the polymer electrolyte membrane fuel cell (PEMFC) is one of the most promising candidates for portable electric power sources because of its lightweight, compactness, high power and low cost. Innovations of modern material sciences and technologies have sped up the development of PEMFC devices during last decade, especially the discovery and application of Nafion membrane as the electrolyte in a fuel cell. Up to the present date, most publications about PEMFC research remain focused on a single cell or emphasized a single part of fuel cell, such as catalysts, membrane, electrode and mechanisms of electrode reactions [2–10]. In order to achieve high voltage and high power, a number of single cells must be assembled together to make a power source for practical applications, and such an assembly is called a fuel cell stack. Most recently, many PEMFC stacks have been

emerging from many developers, revealing a variety of types and functions. However, only a few reports have been published which include an entire fuel cell stack design [11–14]. The present research is to review this variety of PEMFC fuel cell stacks and to explore a logical relationship between the stack structure designs and operational performances. Here, these types of PEMFC stacks will be classified, evaluated and analyzed.

2. Experimental

2.1. Reagents and instrumental

High purity of hydrogen (99.99%) was used as fuel. The temperature and humidity of the fuel cell stacks were controlled with a Tenney Environment Chamber (model No. BTRC), which was programmed through a computer with Linktenn II Software. An Arbin Battery Tester BT-2043 was used for program-controlled PEMFC stack test. A Hewlett-Packard Electronic Load (Model No. 6050A) and a Hewlett-Packard Multimeter were used for measuring stack's current and voltage by non-program control.

2.2. Fuel cell stacks

Several PEMFC stacks were evaluated, which can be classified into three major types of stacks according to the differences of electrode units in the stack design.

^{*} Corresponding author. Tel.: +1-301-721-3451; fax: +1-301-721-3402. E-mail address: dchu@arl.mil (D. Chu).

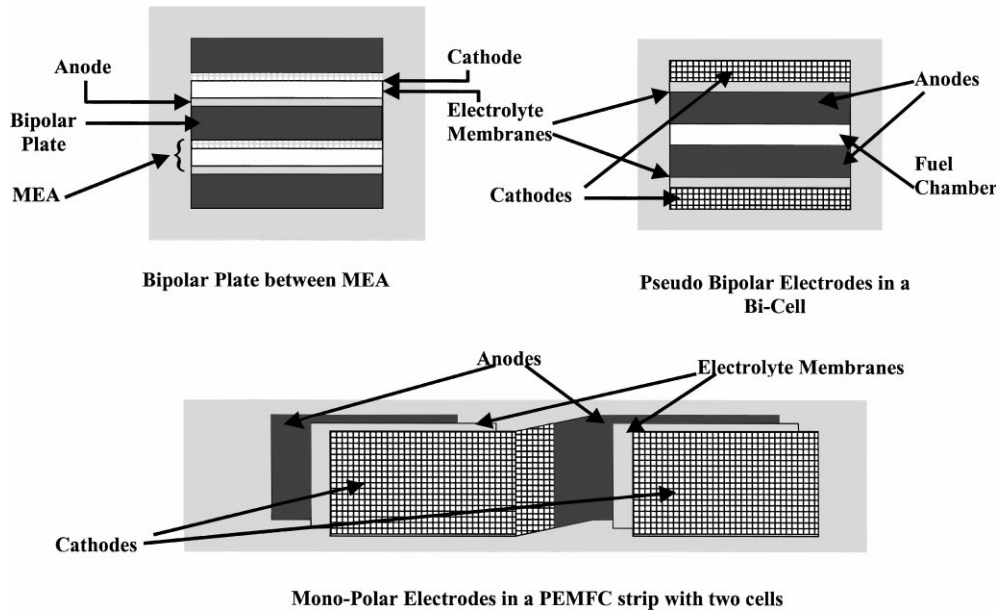


Fig. 1. Schematic drawing of three different types of electrode units in PEMFC.

Fig. 1 shows the schematic plots of these three designs including bipolar, pseudo bipolar and monopolar stacks. Each main type may be further classified into several subtypes based on a specific function designed in the stack system, such as air filling and humidifying styles. Several candidates of the three main types of PEMFC stacks evaluated in our laboratories are briefly described as follows.

1. A 150 W bipolar plate PEMFC stack which used compressed air as oxidant and compressed hydrogen as fuel. This stack had a self-humidifying function and a fan-assisted heat exchange auxiliary. The hydrogen was purged at the outlet automatically.
2. A 50 W bipolar plate PEMFC stack which used pumped air as oxidant and compressed hydrogen as fuel. This stack had a self-humidifying function and a fan-assisted heat exchange auxiliary. The hydrogen was purged at the outlet automatically.
3. A 25 W pseudo bipolar electrode PEMFC stack which used spontaneously convected air as oxidant (air breathing) and compressed hydrogen as fuel. This stack had no self-humidifying function and used spontaneously convected heat exchange.
4. A 100 W pseudo bipolar electrode PEMFC which used fan provided air as oxidant and compressed hydrogen as fuel. This stack had a self-humidifying function and a fan-assisted heat exchange auxiliary.
5. A 12 W monopolar strip PEMFC stack which used spontaneously convected air as oxidant and compressed hydrogen as fuel. This stack had no self-humidifying function and used spontaneous convection heat exchange.

3. Results and discussion

3.1. Bipolar plate stack using compressed air

A bipolar plate stack is assembled from a number of repeated units of membrane electrolyte assembly (MEAs) and bipolar plates like that shown in the upper-left of Fig. 1. The MEA is composed of two electrodes and electrolyte membrane (such as Nafion). The bipolar plate has many flow channels on each side designed for supply of fuel or oxidant. Electricity passes through each bipolar plate, forming electric polarization between both sides. Additional channels or auxiliary functions may be designed for heat exchange and water management. The oxidant generally is air, which may be supplied by compressed or pumped air.

Fig. 2 shows voltage–current and power–current curves of a 150 W bipolar stack using compressed air. The stack had 24 cells, each cell had an area of 42 cm². There is no apparent mass transfer limiting process, because there was no increasing downward slope at the high current region (6–10 A). The open circuit voltage was 23.6 V. The voltage–current curve can be analyzed by two mechanisms, i.e. electrode activation control (mainly at the region before 2 A) and Ohmic control process (mainly at the region from 2 to 10 A), respectively. The performance of the stack can be described with Eq. (1) [12]

$$\sum(E_{i_j}) = \sum(E_{o_j}) \frac{-\log(i) \sum(b_j)}{1000} - \frac{i \sum(R_j)}{1000} \quad (1)$$

where, the subscript j represents the number of a single cell in the stack. For example, if there are N number of single cells in the stack, the $\sum(E_{i_j})$ (V) means the sum of the all single cells' voltage from cell number $j = 1$ to cell number

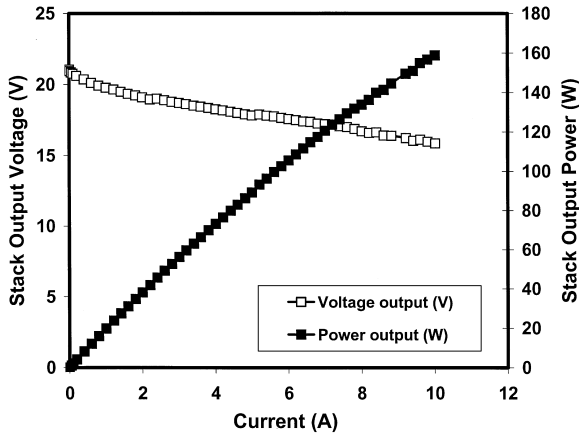


Fig. 2. Voltage and power–current curves of a 150 W bipolar PEMFC stack (24 cells, 42 cm² for each) at 18°C using compressed air.

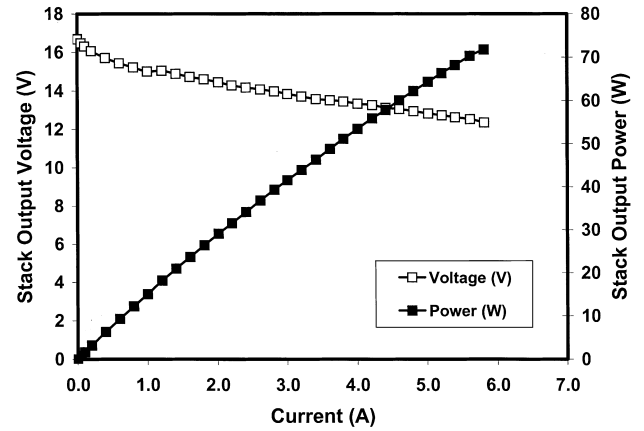


Fig. 4. Voltage and power–current curves of a bipolar PEMFC stack (18 cells, 34 cm² for each) at 20°C and 32% RH using pumped air.

$j = N$. The term $\Sigma(E_{o_j})$ (V) is approximately equal to the open circuit voltage of the stack in volts, and the $\Sigma(b_j)$ is the sum of the Tafel slope (mV/dec) of all single cells in series connection. The $\Sigma(R_j)$ (Ω) is the total electric resistance of the stack. The i is the current value (mA).

The power–current curve was obtained by taking the product of voltage and current of the stack. The short-term maximum power is about 160 W at 10 A, exceeding the 150 W of the stack design goal.

Fig. 3 shows a voltage–time curve at constant current discharge (10 A). The long term performance of the stack meets the design goal of 150 W.

3.2. Bipolar plate stack using pumped air

Fig. 4 shows voltage and power current curves of a 50 W bipolar PEMFC stack using pumped air. There were 18 cells in the stack, each cell had an area of 34 cm². The open circuit voltage is about 17 V, a little lower than the expected 18 V because of a voltage drop from maintaining internal stack operation, to keep the air pump running. There is no

apparent mass transfer process up to 6.0 A, with the short-term maximum power density being about 72 W at 6.0 A. An advantage of using pumped air is that there is no need for a compressed air tank, which is useful to decrease the total weight of stack system.

The stack using pumped air has good long-term discharge performance at low temperature. Fig. 5 shows the voltage–time curves at constant current (4 A) discharge. From 2 to 30°C the discharge curves are relatively stable with power closed to 50 W. At above 40°C the stack can only run a short time and the output voltage drops sharply. The poor performance results at high temperature, because the interior of the stack overheats, which causes the electrolyte membrane to dry out.

3.3. Pseudo bipolar stack using air breathing

The unit of a pseudo bipolar stack is schematically drawn in the upper right of Fig. 1. It looks like the unit of a bipolar

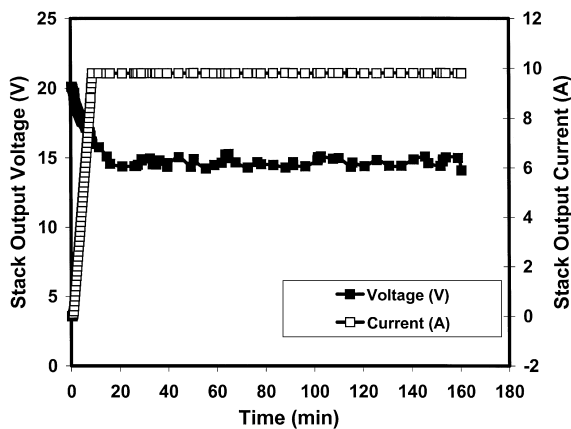


Fig. 3. Constant current discharge performance of a bipolar 150 W PEMFC stack (24 cells, 42 cm² for each) at 18°C using compressed air.

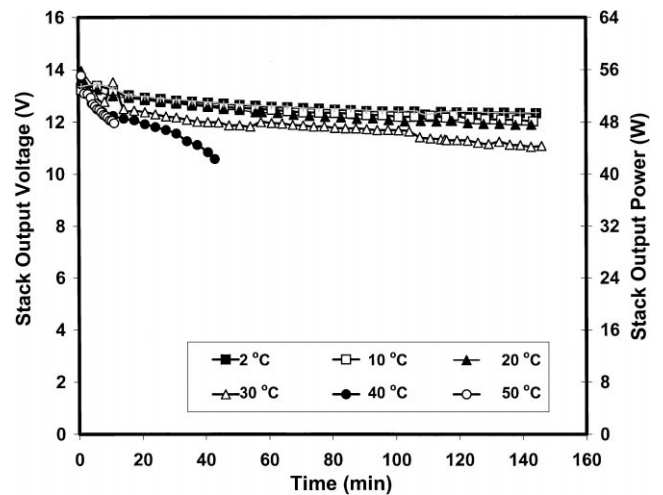


Fig. 5. Constant current (4.0 A) discharge performance of a bipolar PEMFC stack (18 cells, 34 cm² for each) at 60% RH using pumped air.

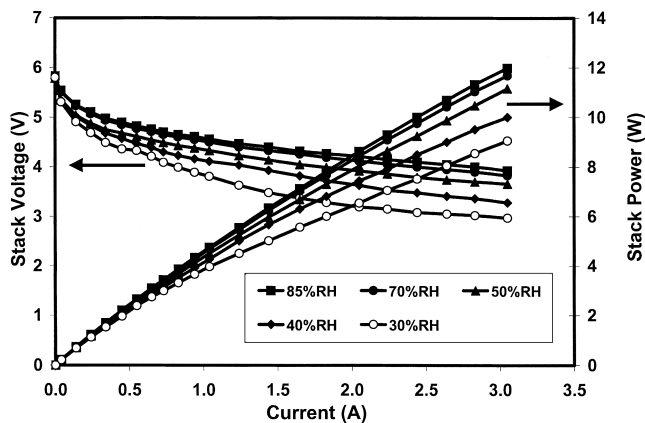


Fig. 6. Voltage and power current curves of a 25 W pseudo bipolar PEMFC stack (six cells, 32 cm² for each) at 35°C using air breathing.

plate stack. However, its true design structure is much different from that of a bipolar. The unit of pseudo bipolar plate contains two cells, with two cathodes at the outsides, two anodes at the insides, which share a common fuel chamber. The performance of pseudo bipolar stack is much different from that of a bipolar stack too.

Fig. 6 shows voltage–current and power–current curves for a 25 W pseudo bipolar stack using air breathing. There were six cells, each cell had an average area of 32 cm². Because this stack did not have a self-humidifying function, its performance is significantly dependent on the environmental humidity. At 85% RH the optimum performance of the stack was obtained. The stack voltage seems to be a function of electrode activation control and Ohmic processes, and apparently dependent on a mass transfer limiting process. The maximum stack power is only about 12 W, less than the expected value for the designed goal. The voltage and power lost can be attributed to cathode limitation because of the insufficient oxygen supply by means of spontaneous convection only. However, the advantage of the pseudo bipolar stack is that there is no need for a bipolar plate, which is tremendously costly in both aspects of materials and processing. Generally, a pseudo bipolar stack is lightweight, low cost and much easier to process as compared with a bipolar stack. With decreasing humidity from 85% RH to 30% RH, the stack performance decreases from 12 to 9 W at 3.0 A.

Fig. 7 shows voltage and power current curves for the stack at various temperatures. From 5 to 35°C it seems that higher temperature results in higher stack performance, because electrode activation plays an important role at these low temperatures. If temperature increases above 40°C, the stack performance no longer increases but decreases in the high current region.

3.4. Pseudo bipolar stack using air fan

In order to improve the cathode performance of the pseudo bipolar stack, an air fan is designed in the stack

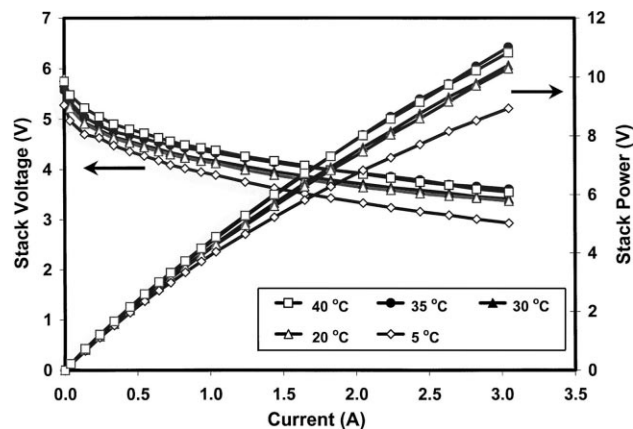


Fig. 7. Voltage and power current curves of a 25 W pseudo bipolar PEMFC stack (six cells, 32 cm² for each) at 50% RH and different temperatures using air breathing.

system to increase oxygen supply from air. Fig. 8 shows voltage and power–current curves of a 100 W pseudo bipolar stack using air fan. The stack had 30 cells. The area per cell was 60 cm². The stack performance is dependent on temperature because electrode activation is faster at higher temperature. The maximum stack performance is obtained at 25°C, giving 9 A with stack power about 165 W, which is far above the designed goal of 100 W.

Fig. 9 shows the voltage and power current curves at 30°C and different relative humidity. From 10% RH to 90% RH the stack performance increases only a little (143–156 W at 8 A).

Fig. 10 shows the voltage–time curve of the stack at constant current (7 A) discharge. The stack voltage is stable via long time operation (>6 h). The stack power is about 140 W, which far exceeds 100 W of designed goal. The operation of the pseudo bipolar stack using an air fan is very convenient because of no need for compressed air.

3.5. Monopolar (strip) stack

Monopolar (strip) stack consists of several strips, in each of which a number of fuel cells are arranged in a line on the same plane. For the reason of simplification and clarification, a strip containing two cells is schematically drawn in the bottom of Fig. 1. These cells are connected in series in each strip by arranging anode and cathode alternatively.

Fig. 11 shows the voltage and power current curves of a 12 W strip-stack at 30°C and different relative humidity. There were 10 cells in the stack, each cell had an average area of 19 cm². Because oxygen is supplied to the stack by spontaneous air convection, the performance of the stack is significantly dependent on the relative humidity. With increasing relative humidity the stack performance increases until water saturation (100% RH) was reached. The strip stack has a high internal resistance because electricity flows along the plane of the strip, which is very different from the bipolar stack, where electric current flows vertically to

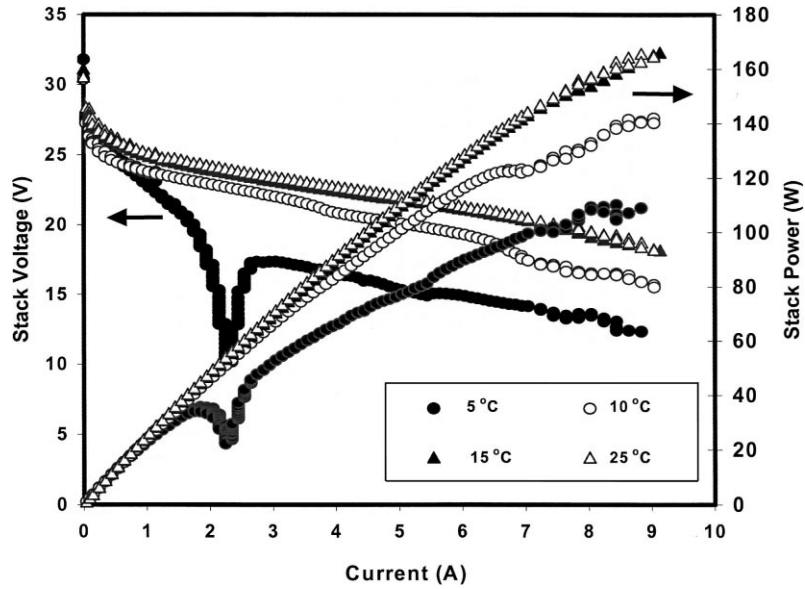


Fig. 8. Voltage and power current curves of a 100 W pseudo bipolar stack (30 cells, 60 cm² for each) at 80% RH using air fan.

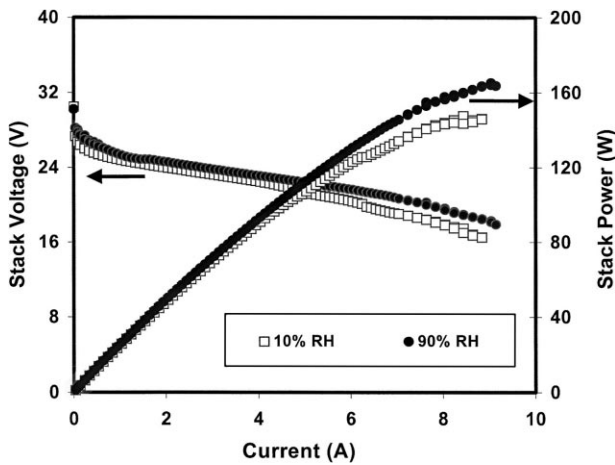


Fig. 9. Voltage and power current curves of a 100 W pseudo bipolar stack (30 cells, 60 cm² for each) at 30°C using air fan.

bipolar plates. The voltage–current curve has an increasing downward slope at the high current region (1.4 A or higher), which is the apparent feature of limiting mass transfer. An empirical equation for describing the voltage and current curve for all processes including electrode activation, Ohmic resistance and mass transfer has been reported in our previous paper [14]

$$E_i = E_o - b \log(1000 i) / 1000 - Ri - i_m m \exp[n i_m] \quad (2)$$

$$i_m = i - i_d \quad (\text{when } i > i_d) \quad (3)$$

$$i_m = 0 \quad (\text{when } i \leq i_d) \quad (4)$$

where, E_i (V) and i (A) are the experimentally measured total voltage of all single cells and current. E_o (V) is the total open circuit voltage for all single cells, and b (mv/dec) is the total Tafel slope of all single cells for oxygen reduction. R (Ω) represents the total Ohmic resistance, such as the

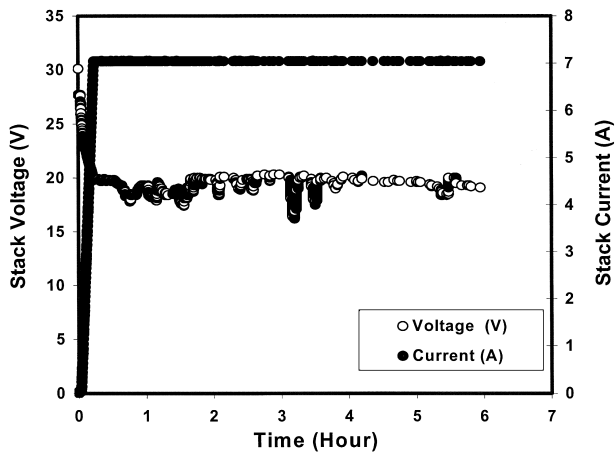


Fig. 10. Constant current discharge of 100 W pseudo bipolar stack (30 cells, 60 cm² for each) at 21°C and 48% RH using air fan.

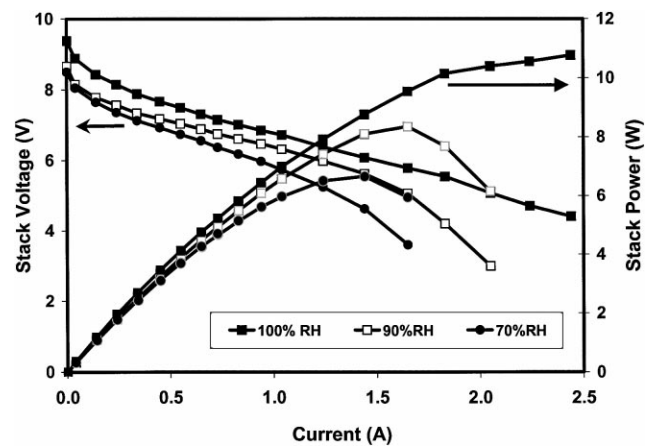


Fig. 11. Voltage and power current curves of a 12 W monopolar stack (10 cells, 19 cm² for each) at 30°C using air breathing.

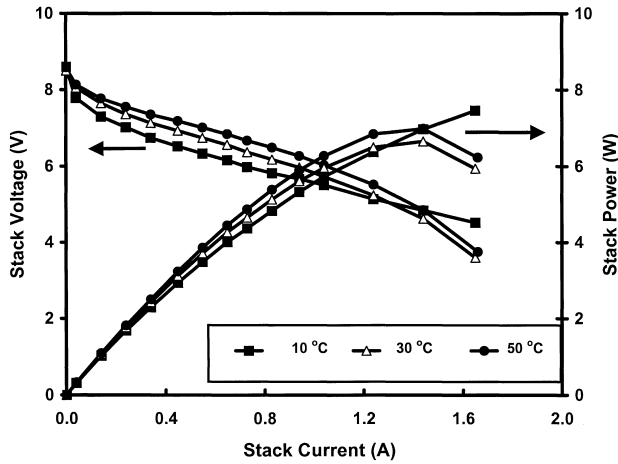


Fig. 12. Voltage and power current curves of a 12 W monopolar stack (10 cells, 19 cm² for each) at 70% RH using air breathing.

resistance of the polymer membrane and electrode components. Here, the i_d is the minimum value of current that causes the voltage deviation from the linearity at the higher current range. The i_d value can be obtained from the experimental curve and from the calculated curve with Eq. (1). The m (Ω) and n (A^{-1}) terms in Eq. (2) are mass-transfer parameters, which can be obtained by fitting the measured voltage–current curve with computer simulation.

The maximum stack power in this case is about 11 W, closed to the expected value 12 W of designed goal. With decreasing relative humidity from 100% RH to 70% RH the stack performance decreases.

The stack performance is also dependent on temperature. Fig. 12 shows voltage and power current curves of the stack at different temperatures. From 10 to 50°C the stack performance increases with temperature at low and middle

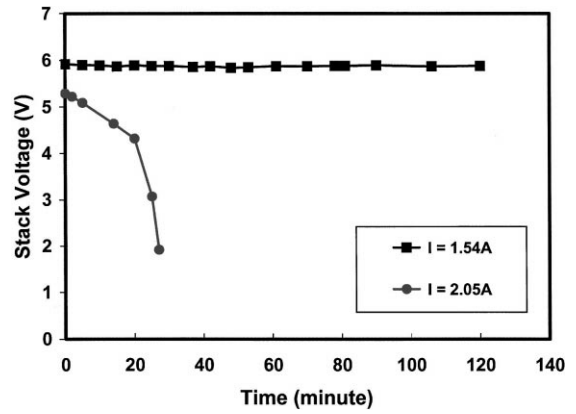


Fig. 13. Constant current discharge performance of a 12 W monopolar stack (10 cells, 19 cm² for each) at 21°C and 100% RH using air breathing.

current region. However, at high current region the performance at 30 and 50°C decreases faster than that at lower temperatures (10°C), because running the stack at high temperature apparently causes electrolyte membrane to dehydrate.

The long-term performance of the stack is demonstrated in Fig. 13. The voltage–time curve of the stack at 1.54 A is very stable within 2 h operation, with long-term output power of 9.2 W. However, when discharge current increases to 2.05 A, the stack can only run for a short term (30 min) and the current decreases sharply. If air fan is used to replace air breathing for air supply the stack performance is expected to improve significantly.

3.6. Characteristics of PEMFC stacks

Table 1 shows a summary of characteristics of three different designs in PEMFC stacks. The bipolar stack has

Table 1
Summary of characteristics of three different designs in PEMFC stacks

Type	Advantage	Disadvantage
Bipolar PEMFC	Each electrode plate serves as anode and cathode in the stack Compact volume, have largest power density by volume Low internal resistance Able to operate at high pressure Rugged	Complex bipolar plate design Heat management required Water management required Complex stack system design High cost of bipolar plates in material and processing Compressed or pumped air is required for oxidant Humidity management required
Pseudo-bipolar PEMFC	Bi-cell is the basic unit in the stack, which is composed of two cathodes on the out sides and two anodes in the inside between which fuel is passing through Middle internal resistance Easy to assemble to high voltage stack with multiple bi-cell units Heat management is easy to be achieved with an auxiliary fan Oxidant (air) can be provided from environment with an auxiliary fan Low cost of electrode material and processing	Need to fill fuel to each bi-cell unit separately Need to link each bi-cell unit electrically
Monopolar (strip) PEMFC	Strip cells are arranged on a same plain Lightweight High voltage of each strip Have largest power density by weight Oxidant (air) can be provided by environment with an auxiliary fan Low cost of electrode materials and processing	High internal resistance Unable to achieve high power by stack system design Fragile

highest power by volume and lowest internal resistance, but its disadvantages are its high cost and complex bipolar plate design. Using pumped air to replace compressed air is useful for decreasing the weight of stack system and for lowering total cost. The pseudo bipolar stack falls in the middle for power density by volume. Its advantage is low cost and ease of fabrication. The monopolar stack has the highest power density by weight. It is easy to achieve high voltage by a single strip. The disadvantage of monopolar design is high internal resistance. In order to achieve optimum performance some specific auxiliary designs in the stack system are needed, such as air flow, humidification and temperature controls.

4. Conclusions

The bipolar stack design is best suitable for a high power supply (from 100 to 1 MW). Water and heat management plays important roles in bipolar stack performance. Pseudo bipolar design is suitable for low to moderate power sources (20–150 W), where humidity management is required. Monopolar design is most applicable to low power and high voltage devices (1–50 W). The performance of monopolar stack is significantly dependent on relative humidity and temperatures.

Acknowledgements

The authors wish to thank the Army Materiel Command for its financial support of this project.

References

- [1] David Linden, *Handbook of Batteries and Fuel Cells*, McGraw-Hill, New York, pp. 41–43, 1984.
- [2] N. Yoshida, T. Ishisaki, A. Watakabe, M. Yoshitake, *Electrochim. Acta* 43 (1998) 3749.
- [3] Y. Sone, P. Ekdunge, D. Simonsson, *J. Electrochem. Soc.* 143 (1996) 1254.
- [4] M.S. Wilson, S. Gottesfeld, *J. Appl. Electrochem.* 22 (1992) 1.
- [5] J. Fournier, G. Faubert, J.Y. Tilquin, R. Cote, D. Guay, J.P. Dodelet, *J. Electrochem. Soc.* 144 (1997) 145.
- [6] E. Passalacqua, F. Lufrano, G. Squadrito, A. Patti, L. Giorgi, *Electrochim. Acta* 43 (1998) 3665.
- [7] O. Antoine, Y. Bultel, R. Durand, P. Ozil, *Electrochim. Acta* 43 (1998) 3681.
- [8] D. Chu, *Electrochim. Acta* 43 (1998) 3711.
- [9] K.Y. Chen, A.C.C. Tseung, *J. Electrochem. Soc.* 143 (1996) 2703.
- [10] P.K. Shen, K.Y. Chen, A.C.C. Tseung, *J. Electrochem. Soc.* 142 (1996) 85.
- [11] O.J. Murphy, A. Cisar, E. Clarke, *Electrochim. Acta* 43 (1998) 3829.
- [12] D. Chu, R. Jiang, *J. Power Sources* 80 (1999) 226.
- [13] D. Chu, R. Jiang, *J. Power Sources* 83 (1999) 128.
- [14] D. Chu, R. Jiang, C. Walker, *J. Appl. Electrochem.* 30 (2000) 365.